Materials Research Proceedings 28 (2023) 1075-1082 https://doi.org/10.21741/9781644902479-118

Modelling of the weld seam in the forming simulation of friction stir welded tailored blanks

BACHMANN Maximilian[1,a *], RIEDMÜLLER Kim[1,b], LIEWALD Mathias[1,c] and MERTEN Mathias[2,d]

[1]Institute for Metal Forming Technology, Holzgartenstraße 17, 70174 Stuttgart, Germany

[2]DYNAmore GmbH, Stralauer Platz 34, 10243 Berlin, Germany

[a]maximilian.bachmann@ifu.uni-stuttgart.de, [b]kim.riedmueller@ifu.uni-stuttgart.de, [c]mail@ifu.uni-stuttgart.de [d]mathias.merten@dynamore.de

Keywords: Tailor Welded Blanks, Material Modelling, Sheet Forming

Abstract. In former papers methods to join different aluminium or different steel plates having same thicknesses are presented. These blanks are often joined by friction stir welding using flat tools. In order to increase the lightweight potential, the Materials Testing Institute of the University of Stuttgart developed a modified friction stir welding process to join aluminium and steel plates of different thicknesses. The process differs from the conventional method in stir welding tool used, which consists of a stepped welding pin and enables combined lap-and-butt joints to be produced. In this paper, a suitable material model is presented to describe this weld seam, allowing the forming behavior of hybrid sheet metal compounds to be realistically simulated.

Introduction

In car body construction, lightweight design approaches are becoming more common, in which weight of components is reduced by substituting one material by a comparatively lighter material (lower density). On the one hand, the weight reduced this way can extend the range of vehicles, which is particularly important in terms of the future or acceptance of electromobility, as charging cycles per kilometre driven play a significant role. On the other hand, lightweight components contribute to regulatory compliance as they lead to a reduction in the CO_2 footprint of vehicles by lowering the energy consumption to drive the vehicle and by requiring less material to be used in production [1]. One challenge arising in the substitution of known materials consists in the required adaptation of the component geometries and the joining processes used [2]. When combining high-strength aluminium alloys or even combinations of aluminium and steel alloys lightweight construction potentials increases. In particular, joining processes established in car body construction, such laser beam and resistance spot welding, show limitations regarding the combination of such materials.

Sheet metal components made of different high-strength aluminium alloys and different sheet thicknesses can be used in the same applications as conventional materials, providing better properties like higher strength and lower density. However, joining of such high-strength aluminium alloys (e.g. 6000-series alloys) by established joining processes such as laser beam welding proves to be difficult due to the materials' tendency to hot cracking during or after welding [3]. In addition, the high heat input of the laser beam welding process causes a reduction of the strength of aluminium alloy, resulting finally in a reduced strength of the joint (weld seam) [4]. For resistance spot welding, high wear of electrodes poses a problem when welding such materials. These problems in joining high-strength aluminium alloys were circumvented in 1991 with the friction stir welding process patented by Thomas et al [5]. In this process, the process energy required is introduced by means of a rotating welding tool, which is pressed into and moved along the joint gap [6]. Since the melting temperature is principally not reached during friction stir

welding due to the method of energy input, the materials to be joined remain in the solid phase during the entire process. Joining of different sheet materials with different sheet thicknesses allows application-specific lightweight solutions to be realized. When joining different sheet materials with different sheet thicknesses, however, the welding tool in general has to contact the joint area flatly. Furthermore, for the joining of aluminium and steel, a joining method is required that minimises the appearance of intermetallic phases, as these reduce the strength of the weld seam, and at the same time the surface of the steel is sufficiently activated to form the joint with the aluminium. To ensure this, the Materials Testing Institute of the University of Stuttgart (MPA) developed a variation of the friction stir welding process to join different aluminium or aluminium and steel blanks of different thicknesses. In this process a combined overlap and butt joint is used as shown in Fig. 1. Here, the thicker metal sheet is provided with a milled step in sheet thickness into which the thinner sheet is inserted before the stir welding process [7].

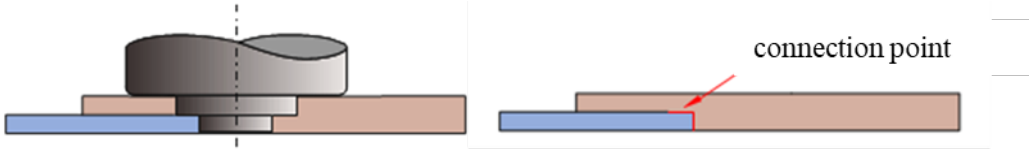

Fig. 1. Combined lap and butt joint; left: with welding tool, right: connection point [1].

Design of the pin of the welding tool shown in Fig. 1 is shaped in a way that both the front face and the surface of the steel sheet are activated. Additional the tool shoulder only rests on the aluminium and therefore does not rub on the steel as with conventional butt joints. The tool live, especially of the tool shoulder significantly is increased. The presented friction stir welding process can therefore be used both to join high-strength aluminium alloys and to produce mixed aluminium-steel joints [8,9]. The use of mixed aluminium-steel joints has a considerable potential for lightweight materials, as load-adapted components can be produced in which higher stressed sections can be provided with a steel sheet and the remainder with an aluminium sheet. In addition to the possibility of joining different materials of different sheet thicknesses, the developed welding process serves as solution annealing. Components of different materials, sheet thicknesses and material grades manufactured with friction stir welding are known as Tailor Welded Blank (TWB).

Previous studies [10] show that TWBs made of aluminium and steel having the same sheet thickness of the base materials show relatively good forming properties as cups with drawing depths similar to the base materials could be drawn. However, [10] considered only 5000-series alloys on the aluminium side in his investigations. Singar [11] investigated the forming capacity of aluminium-steel TWBs made of HX340LAD (0.8mm) and AA 6014 T4 (1.2mm) joined by the cold metal transfer welding process. However, the investigations shown, that the values achieved for elongation at break (approx. 7%) and forming limits from the forming limit diagram required further work to produce TWBs suitable for industrial use.

By using the friction stir welding process presented in this paper hybrid TWBs consisting of DX54 (1.0 mm) and AA 6016 T4 (2.0 mm) can be produced showing a new potential for forming operations [12]. For these hybrid TWBs a simulative mapping approach is developed with focus on the question how the hybrid TWB has to be modelled in order to describe the forming process realistically. First the material characterization in form of tensile tests and the determination of the forming limit curves is carried out for the base materials and the weld seam. With the results from these characterizations a simulative approach of TWBs is set up by mapping the properties of the three components aluminium, steel and weld seam in separate parts in order to map the forming behaviour and thus increase acceptance of aluminium-steel TWBs in the industry.

Material Characterization

For deriving the material model for the forming simulation, the mechanical properties and the forming limit curves (FLC) of both the base materials (DX54 and AA6016 T4) and the weld seam of the TWBs were determined. Concretely, tensile tests were performed at the DYNAmore GmbH to obtain yield curves and Nakajima tests were carried out at the Institute for Metal Forming Technology (IFU) for determining the FLCs. The weld seam was furthermore characterized by the area of the combined lap and butt joint. The yield curves measured via the tensile tests are shown in Fig. 2. Here, for the base materials specimens were testes with 0°, 45° and 90° to rolling direction and for the weld seam, specimens were tested with 0° and 90° to the welding orientation. Each characterization test was performed using 5 samples. The extrapolation of the data from the tensile test was done using Hockett-Sherby. In Fig.2 the yield curves for AL6016 T4 and DX54 in 0° are presented as these are the rolling directions with the lowest loading limits. In this context, Fig. 2 shows the flow curve of the weld seam specimen taken 0° to the welding orientation which is above the flow curve of the base material AA6016 T4, but below the flow curve of the base material DX54. In contrast, the yield curve of the weld seam taken 90° to the welding orientation is below the yield curve of both base materials. Considering these properties, it can be seen weld seams should be positioned in 0° to the welding orientation in order to obtain components with a correspondingly strength.

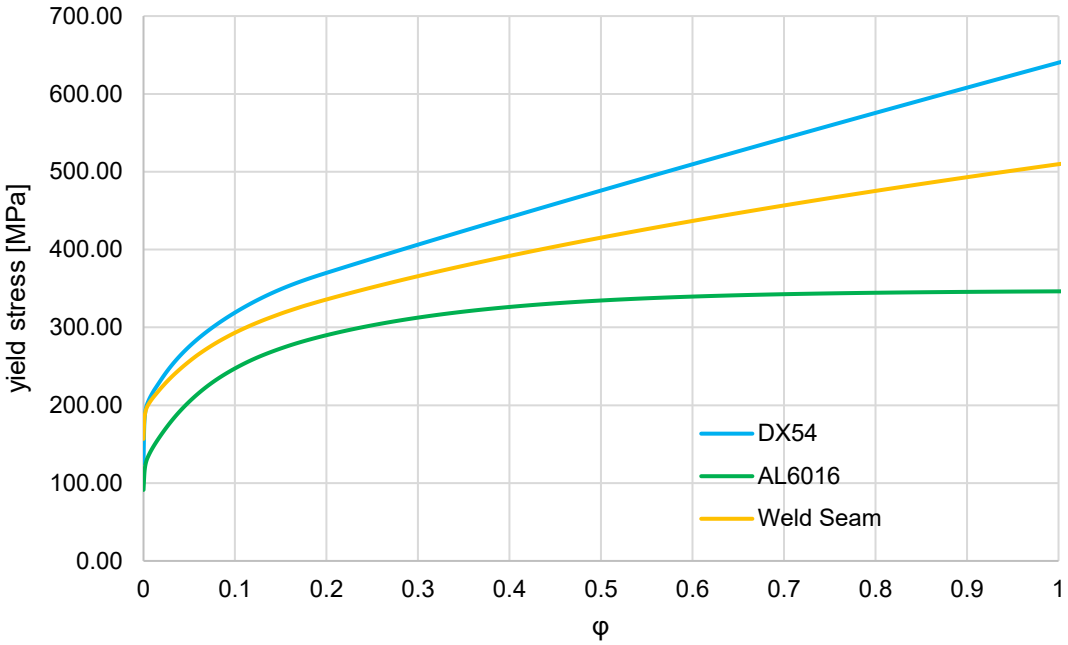

Fig. 2. Yield curves of AA6016 T4, DX54 and weld seam.

The forming limit curves of the TWBs were determined on the basis of 5 support points (waist of 30 mm, 60 mm, 100 mm, 140 mm and 200 mm) according to ISO 12004 [13] using a workshop press of the IFU (see Fig. 3, left and middle). For each of the 5 support points, Nakajima specimens were produced with a welding orientation of 0° and 90°. Each support point was determined using 4 valid samples. The smaller sheet thickness of the aluminium sheet of the TWB was compensated by means of a shim plate, thus ensuring a uniform force application during the testing procedure. The phenomenon of weld seam migration during forming in the direction of the aluminium could be minimized by increasing the pressure of the gas springs of the blank holder.

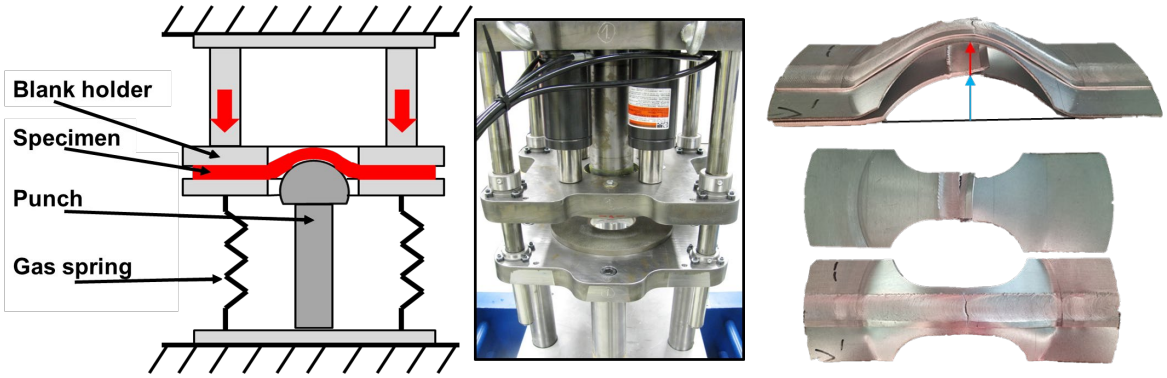

Fig. 3. Principal of the Nakajima test used (left), Nakajima testing device at IFU (middle), TWBs with a welding orientation of 0° and 90° (right).

Depending on the weld direction in the specimens, different results were observed with regard to crack initiation. For the specimens with 0° welding orientation, the crack forms, as usual for Nakajima tests of monolithic specimen, starting from the weld in the middle in the direction of the sheet edge (Fig. 3, right bottom). In this case, the load applied by the punch is absorbed by the weld seam and the base materials. Here, the GOM aramis system could be used to determine the major and minor strains before cracking. Determining the crack initiation for specimen with a welding orientation of 90° proved more difficult. Here, the failure was also initiated in the weld seam, but could not be identified as a local crack on the upper side of the sheet. The applied force of the punch is absorbed only from the weld seam which forces the weld seam to open up from the bottom side of the sheet. Therefore, no crack could be detected on the upper side of the sheet. On the upper side of the sheet only the separation of the weld seam was detected, (see Fig.3 right, middle). In this case, the crack initiation moment could be determined from the history curve of the major and minor strain, since they showed a rapid decrease after separation of the sheets due to the force of the punch. This moment was defined as the crack initiation moment for TWB with welding orientations of 90°.

The different forming behavior of TWBs considering the welding orientation is shown in Fig. 3 (right, top), illustrating the lateral plan view of Nakajima specimens with a waist of 30 mm. The drawing depth at 90° welding orientation is given in blue and the drawing depth at 0° welding orientation is shown in red. Such differences in the forming capability of the TWB could be observed for all waists and are shown in the forming limit diagram for both cases (0° and 90° orientation of the welding seam) in Fig. 4.

Comparison of the two FLCs reveals that TWBs show different forming capability depending on the weld orientation for each loading condition (uniaxial, plain strain, biaxial). These results correspond to those from the tensile tests already presented, as the forming capability of TWBs with a welding orientation of 90° is below the forming capability of 0° at the critical plane strain load.

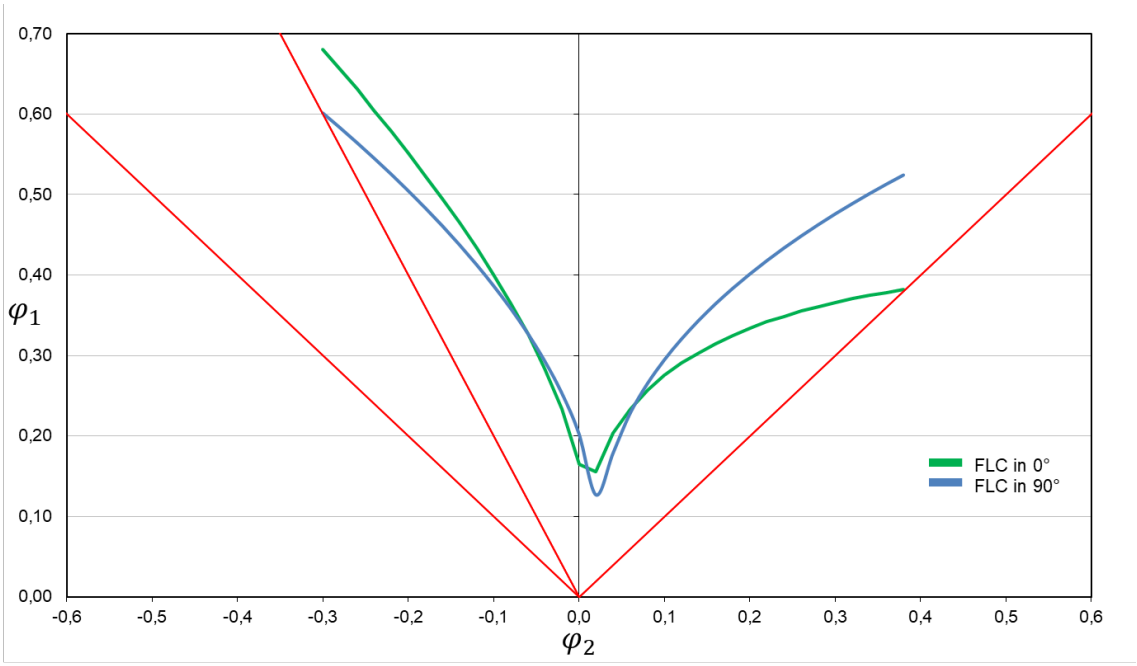

Fig. 4. Forming limit diagram for DX54/AL6016 TWBs in 0° and 90° welding orientation.

Numerical Simulation Setup

The mechanical properties determined for the base materials DX54 and AA6016 T4 as well as the weld seam were subsequently used to set up material models for the simulation of a Nakajima test performed. As described before the failure behavior varies due to the welding orientation and in this approach the welding orientation of 0° was further investigated. The simulations aimed to model the forming behavior of the TWB specimen with different waists and welding orientation of 0° during the Nakajima test as accurately as possible. For simulation setup and performing, the simulation software DYNAFORM and LS-PREPOST were used. Previous simulation work in this field was mainly concerned with the modeling of TWBs consisting of the same material using the software ABAQUS [14], TWBs consisting of different aluminium alloys [15] or TWBs produced by laser welding [16]. In laser-welded TWBs, the width of the weld seam is only a few millimeters compared to friction stir welded TWBs. Moreover, the higher process temperatures of laser welding as opposed to friction stir welding lead to significantly differing forming behavior, especially of the weld seam but also of aluminium sheets as part of a TWB. To account for these characteristics, a new modeling approach was developed for the numerical study on the forming behavior of friction stir welded TWBs presented in this paper, distinguishing it from previous work on laser welded TWBs. The distinction from [14] and [15] is made by considering different materials (aluminium and steel) with different thicknesses. In contrast to [17] this modelling approach on the one hand considers anisotropic material behavior and on the other hand describes the weld seam not only by node definitions, but as an independent material with its specific forming behavior.

In the model approach, the welded blank was divided into three parts (the aluminium side, the weld seam and the steel side) as shown in Fig. 5 a). The weld seam was designed with a width of 20 mm, which corresponds to the area of the combined lap and butt joint of the real TWB. The interface from AA6016 T4 to the weld seam and from the weld seam to DX54 were modeled using the weld function of DYNAFORM. Normally, failure values are assigned to these weld functions to implement the failure behavior at this location. However, as shown during the Nakajima tests, the TWB considered did not fail on the interfaces between the base materials and the weld seam, but within the weld seam. For this reason, the weld function was assigned with ‘no failure’. Each of the three parts was assigned with its determined mechanical properties using the material model

MAT_036-3-Parameter_Barlat. The entire welded blank was meshed with shell elements having a size of 1 mm, which means the weld seam has been represented with 20 elements in width. Fig. 5 b) shows the entire simulation setup with punch, blank holder, die and TWB in lateral plan view.

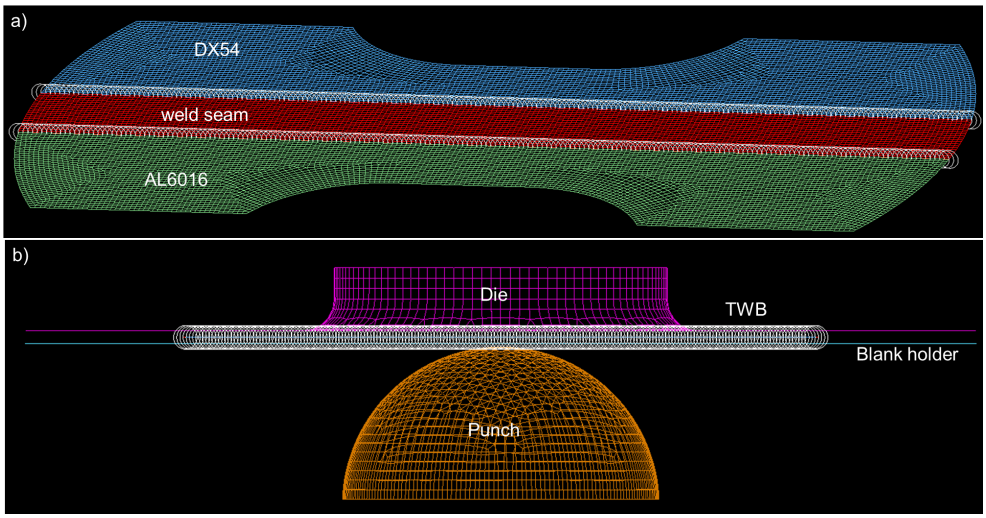

Fig. 5. a) Separation of the blank in 3 parts; b) Simulation setup of Nakajima test considered.

Validation Of Simulation Model

For validation of the simulation results, the strain values measured in the corresponding Nakajima test were compared with the strain values calculated from the simulation. Furthermore, by importing the forming limit curve for the welding orientation of 0°, the crack initiation moment was determined based on the simulation results and compared with the crack initiation observed in the experiment. In this context, Figure 6 shows the major strain distribution of a Nakajima specimen with a waist of 60 mm calculated by simulation on the left side and measured in the experiment on the right side. On the right side the measurement results from the experiment of three samples are shown. The average value for the major strain at crack initiation moment is $\varphi_1 = 0{,}283$ in contrast, the simulative determined main strain is $\varphi_1 = 0{,}31$. Comparison of these strain results revealed the strain distribution could be calculated quite accurately with the established simulation model for TWB consisting of DX54 and AA 6016 T4, but the strain values at crack initiation were overestimated relative to the strain values measured in the experiment. In Fig. 6 the location of crack initiation is highlighted with black arrows. The simulation differs slightly from the experiment with respect to the predicted location of crack initiation. The simulation result indicates this allocation slightly closer to the transition between the weld seam and the base material. The reason for these deviations in the simulation is probably the weld seam exhibits a different mixture of aluminium and steel in the transition area to the base materials compared to the weld seam center. This was not considered in the characterization tests of the weld seam carried out so far.

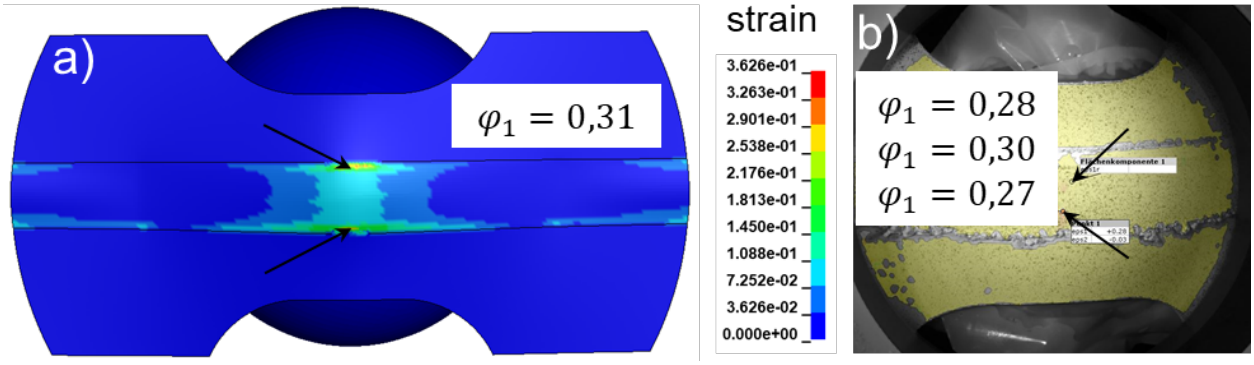

Fig. 6. Strain values before crack initiation moment a) major strain in simulation, b) major strain in experiment.

Summary

In this paper, a modelling approach for the numerical forming simulation of TWBs with a special focus on the consideration of the weld seam is presented. First, the base materials DX54 and AA6016 T4 as well as the weld seam of the TWB considered were characterized. Based on these tests, a simulation model of one of the Nakajima tests was set up and validated using the strains numerically calculated and experimentally measured. The simulation results revealed that the forming behavior of the TWBs could be described quite accurately by mapping the properties of the three components aluminium, weld and steel separately, but the behavior of the weld seam still needs to be represented in more detail as the predicted location of crack initiation varies from the experiments.

In the future, in addition to the strain values, the force curves from simulation and experiment will be compared to base validation on 2 values. Furthermore, a simulative representation of the weld seam with shell and volume elements will be aimed in order to implement hardness measurements of the weld seam in the simulation and thus to consider the transition of the weld seam to the base materials in more detail. Possible variations of the properties of the weld seam will thus considered in further investigations by implementing the hardness profile of the weld seam and linking it to a prior damage. In addition, other connection methods will be considered to map the crack initiation at the correct location. Moreover, simulation of the Nakajima test with welding orientation of 90° will be considered in the future as they have a different failure behavior which was described in this work.

Acknowledgement

The work of this paper was carried out within the framework of the project CO2-HyChain, which is funded by the Technologietransfer-Programm Leichtbau (TTP LB) of the Federal Ministry of Economic Affairs and Climate Action.

References

[1] A. Birkert, S. Haage, M. Straub, Umformtechnischer Herstellung komplexer Karosseriebauteile – Auslegung von Ziehanlagen. Springer Verlag Berlin Heidelberg, 2013.

[2] F. Henning, E. Moeller, Handbuch Leichtbau – Methoden, Werkstoffe, Fertigung. Carl Hanser Verlag München Wien, 2020.

[3] M.W. Mahoney, C. Rhodes, J.G. Flinott, W.H. Bingel, RR. Spurling, Properties of friction stir-welded 7075 T651 aluminium, Metall. Mater. Trans. A 29 (1998) 1955-1964. https://doi.org/10.1007/s11661-998-0021-5

[4] A.K. Lakshminarayanan, V. Balasubramanian, K. Elangovan, Effect of welding processes on tensile properties of AA 6061 aluminium alloy joints, Int. J. Adv. Manuf. Technol. 40 (2009) 286-296. https://doi.org/10.1007/s00170-007-1325-0

[5] W.M. Thomas, E. Nicholas, J. Needham, M. Murch, P. Temple-Smith, C.J. Dawes, Great Britain Patent Application No. 9125978.8 (1991).
[6] H.B. Schmidt, J.H. Hattel, Thermal Modelling of friction stir welding, Scirpta Mater. 58 (2009) 332-337. https://doi.org/10.1016/j.scriptamat.2007.10.008
[7] M. Werz, Experimentelle und numerische Untersuchungen des Rührreibschweißens von Aluminium- und Aluminium-Stahl-Verbindungen zur Verbesserung der mechanischen Eigenschaften, Materialprüfungsanstalt (MPA) Universität Stuttgart, Dissertation, 2020.
[8] T. Wanatabe, H. Takayama, A. Yanagiswa, Joining of aluminium to steel by friction stir welding, J. Mater. Process. Technol. 178 (2006) 342-349. http://doi.org/10.1016%2Fj.jmatprotec.2006.04.117
[9] H. Uzun, C. Donne, A. Arganotto, T. Ghidini, Friction stir welding of dissimilar AL 6013-T4 to X5CrNi18-10 stainless steel, Mater. Des. 26 (2005) 41-46. https://doi.org/10.1016/j.matdes.2004.04.002
[10] T. Tanaka, T. Hirata, N. Shinomiya, N. Shirakawa, Analyses of material flow in sheet forming of friction-stir welds on alloys of mild steel and aluminium, J. Mater. Process. Technol. 22 (2015) 115-134. https://doi.org/10.1016/J.JMATPROTEC.2015.06.030
[11] O. Singar, M. Merklein, Study on the formability characteristics of the weld seam of Aluminium Steel Tailor Hybrid Blanks, Key Eng. Mater. 549 (2013) 302-310. https://doi.org/10.4028/www.scientific.net/KEM.549.302
[12] F. Panzer, M. Schneider, M. Werz, S. Weihe, Friction stir welded and deep drawn multi-matieral tailor welded blanks, Materials Testing, Carl Hanser Verlag, München, 2019.
[13] DIN Deutsches Institut für Normung e.V., Metallische Werkstoffe – Bestimmung der Grenzformänderungskurve für Bleche und Bänder – Teil 2: Bestimmung von Grenzformänderungskurven im Labor, Beuth Verlag GmbH, Berlin, 2021.
[14] W. Lee, K.-H. Chung, D. Kim, J. Kim, C. Kim, K. Okamoto R.H. Wagoner, K. Chung, Experimental and numerical study on formability of friction stir welded TWB sheets based on hemispherical dome stretch tests, Int. J. Plast. 25 (2009) 1626–1654. http://doi.org/10.1016/j.ijplas.2008.08.005
[15] C. Leitao, B.K. Zhang, R. Padmanabhan, D.M. Rodrigues, Influence of weld geometry and mismatch on formability of aluminium tailor welded blanks: numerical and experimental analysis, Sci. Technol. Weld. Join. 16 (2011) 662–668. https://doi.org/10.1179/1362171811Y.0000000055
[16] X. Qiu, The study on Numerical Simulation of Tailor Welded Blanks in Square Cup Stamping, Adv. Mater. Res. 189-193 (2011) 3932-3935. https://doi.org/10.4028/www.scientific.net/AMR.189-193.3932
[17] O. Singar, D. Banabic, Numerical Simulation of Tailored Hybrid Blanks, Proceedings of Romanian Academy, Sereis A, Volume 22, Number2/2021, pp. 177-184.